

V Riccardo et al

Modelling Magnetic Forces during Asymmetric Vertical Displacement events in JET

Modelling Magnetic Forces during Asymmetric Vertical Displacement Events in JET

V Riccardo¹, S Walker², P Noll.

JET Joint Undertaking, Abingdon, Oxfordshire, OX14 3EA,

¹Present address: UKAEA Fusion, Culham, UK.

²Imperial College, London, UK.

Preprint of a Paper to be submitted for publication in
Fusion Engineering and Design

January 2000

"This document is intended for publication in the open literature. It is made available on the understanding that it may not be further circulated and extracts may not be published prior to publication of the original, without the consent of the Publications Officer, JET Joint Undertaking, Abingdon, Oxon, OX14 3EA, UK".

"Enquiries about Copyright and reproduction should be addressed to the Publications Officer, JET Joint Undertaking, Abingdon, Oxon, OX14 3EA".

ABSTRACT

Asymmetric vertical disruption events (AVDEs) are fortunately rare, but can induce large lateral forces which can cause significant mechanical damage to tokamaks. In this paper we present a simple model which allows the lateral forces generated during such a disruption to be estimated as a function of relatively easily obtained electromagnetic parameters: the asymmetries in the vertical current moment. This model is validated by using it to predict the displacement history of the JET tokamak caused by a number of major AVDEs. It is shown that the predicted forces and displacements agree well with quantities measured during these disruptions. One conclusion from the model is that the maximum sideways displacement scales with the product of the plasma current and the toroidal field, and this recipe is now used at JET to assess a priori the hazards of performing high current and high field pulses when they are known to be likely to disrupt.

1. INTRODUCTION

Plasma disruptions and vertical displacement events (VDEs) are a threat to present and future fusion experimental devices [1]. Asymmetries can exacerbate the dangerous effects of the thermal and electromechanical disruption loads and have to be taken into account in defining the operational space of present tokamaks and in designing future ones.

The characteristics of the disruption asymmetries depend strongly on the machine. Their cause can be in small geometrical asymmetries of the structures or in the plasma. In JT60-U the presence of asymmetries is derived from cyclical divertor tile damages, which suggests a link with toroidal field asymmetry [2]. Similarly, in COMPASS [3] the toroidal mode $n=1$ seems to appear preferentially at a fixed location, which can be explained by a vessel assembly unisotropy. In [3] the asymmetry parameters are estimated using halo current measurements, and this is the most commonly used technique to detect plasma asymmetries during disruptions. Halo currents are currents flowing from the open field line region of the plasma periphery into (and out of) the first wall. Plasma asymmetries can produce a Toroidal Peaking Factor (TPF) of the halo current as large as 2.5 in DIII-D, however in the same device the use of killer pellets reduces the TPF 1.6-2.0 [4]. The dynamic behaviour seems to depend on the electrical characteristics of the vessel wall: DIII-D asymmetries seem to rotate slowly, those of Alcator-C [5] rotate at a few kHz and both in Asdex-Upgrade [6] and at JET they are locked. It is the unusual flexibility of the JET vessel system, together with the tendency of JET asymmetries to lock, that makes this tokamak an interesting subject for studies for asymmetric disruptions. The JET vacuum vessel moves significantly in response to the net horizontal forces produced during locked asymmetric vertical displacement events (AVDEs). Measurements of displacement are reliably available in several positions around the JET vessel [7] and can be used to evaluate theories which aim to predict the net horizontal force from measured plasma parameters.

An analytical model which aims to predict the net radial force produced during a toroidally asymmetric disruption on the structure of a tokamak is presented and validated in this paper.

This magnetic force model is a development of an earlier one [8], and incorporates modifications to make it of wider applicability.

The model is based on analysis of the asymmetric magnetic fields around the plasma, which is represented as a current filament, as it is displaced asymmetrically during a disruption. From a knowledge of these measured magnetic quantities the model permits the forces acting on the plasma and vessel to be computed.

In this paper we describe this magnetic force model, and use it, in conjunction with a mechanical model of the vessel's response to impulsive loadings, to predict the displacement history of the vessel during a number of disruptions. These predictions are then compared to those actually observed during these disruptions, to validate the magnetic model.

The structure of the paper is as follows. In section 2 the phenomenology of AVDEs is discussed. The analytical magnetic force model of the forces on the plasma and vessel, and the simplification implemented in the present paper, are presented in section 3. The experimental measurements, of both the magnetic quantities and displacements, and their processing, are described in section 4. In section 5 the mechanical model used in the validation of the dynamic response of the structure is described in some detail, and its sensitivity to uncertainties investigated. Section 6 addresses validation of the magnetic force model, validating in stages the prediction of the direction of displacement, the proportionality of the observed displacement to the postulated electromagnetic parameters, and finally the actual transient displacement histories.

2. ASYMMETRIC VERTICAL DISPLACEMENT EVENTS (AVDES)

Vertical displacement events (VDEs) denote disruptions characterised by large vertical movements of the plasma while its current remains more or less undiminished. During these events halo currents provide a force on the plasma that balances the destabilising force caused by the loss of the equilibrium vertical position [9]: the vertical force on the vessel due to the halo currents is equal and opposite to the one acting on the plasma and it is mainly due to the interaction of the poloidal component of the halo current with the toroidal magnetic field.

Occasionally this movement has been found asymmetric in JET: the plasma vertical displacement differs in magnitude and direction between toroidal locations, and can be accompanied by a horizontal displacement. In JET such VDEs generally lock, and these locked asymmetric VDEs (AVDEs subsequently) are associated with the largest electromagnetic loadings of the JET vacuum vessel and its attachments. Although at JET AVDEs are fortunately rather rare (typically one in every 10 VDEs, and VDEs themselves only occur about one in any 10 pulses) they can be damaging. The largest sideways displacement recorded so far in the operation of JET is a 7.1 mm lateral displacement, during a disruption that produced a peak of 700 kN net radial force on the main vertical port (MVP) supports and a 800 kN force on the hydraulic dampers at the main horizontal ports (MHPs). Another produced a 5.6 mm lateral displacement in the direction of one of the neutral beam injectors and damaged the vacuum seals of the valve

between the torus and that neutral beam box. Subsequently the valve had to be refurbished and extra lateral supports at the MHPs added.

For a JET vertical instability to progress into an AVDE requires both that the plasma current does not begin to decline until the plasma displacement is significant, and that as the plasma cross section shrinks, the safety factor at the boundary becomes low enough for the onset of the MHD instability. Once the asymmetry has started the plasma current and position appear to be toroidally non-uniform in a fashion resembling a mode $m=1/n=1$ configuration.

It has long been known qualitatively that AVDEs generate large net horizontal (sideways) forces on the JET vacuum vessel, which in turn moves sideways and can cause mechanical damage. During these events the plasma-vessel force balance is provided mainly by the asymmetric fraction of the halo currents recirculating in the vessel with path not parallel to the field lines. However, a clear understanding of the causes and mechanisms of AVDEs is still missing. At JET AVDEs seem to be a mode $m=1/n=1$ instability made possible by a low boundary safety factor; but other interpretations of the phenomenon, involving special plasma-wall eigenmodes that have no direct counterpart in the plasma itself [10] or non-uniform first wall geometry [11] as sources for the fuelling of the asymmetry, have been put forward.

3. SIMPLE ANALYTICAL MODEL OF AVDE MAGNETIC FORCES ON THE VESSEL

It is possible to construct a simple analytical model of an AVDE, and in particular of the forces it induces in the vacuum vessel and associated structure. This description builds upon and is a simplification of the model outlined in [8].

In essence, the model permits the estimation of the time dependent lateral force on the vessel during the course of the AVDE, primarily as a function of the time dependent difference between the vertical current moments on opposite sides of the torus.

The plasma is represented by a rigid current carrying ring with major radius R_0 , minor radius a and toroidal current I_0 . As suggested by measurements of the current centroid position, the current ring is assumed to be shifted by Δx along the x -axis and tilted about that axis by a small angle $\alpha=\Delta z/R_0$, as indicated in Fig.1. The toroidal field gives rise to a force at the current ring in the x -direction and to a torque about the x -axis with the same polarity as the assumed tilt α . The force can be calculated as follows.

In the frame moving with the current ring the component of the magnetic field can be expressed as a function of R , φ and z . To the first order in the small quantities α and Δx one finds

$$B_R \approx B_0 R_0 (\Delta x \sin \varphi - \alpha z \cos \varphi) / R^2$$

$$B_\varphi \approx B_0 R_0 (R - \Delta x \cos \varphi - \alpha z \sin \varphi) / R^2$$

$$B_z \approx B_0 R_0 \alpha \cos \varphi / R$$

where B_0 is the original toroidal magnetic field at the radius R_0 , and the location of a current ring element δI_0 inside the cross section πa^2 is defined by R, z . The force in x -direction acting on the current element becomes

$$\delta F_x = \oint \delta I_0 B_z(R, \varphi) \cos \varphi R d\varphi \approx \pi \delta I_0 B_0 R_0 \alpha.$$

This is independent of R, z to the first order. The total force acting on the current I_0 through the toroidal magnetic field is therefore

$$F_x \approx \pi I_0 B_0 R_0 \alpha = \pi I_0 B_0 \Delta z.$$

Poloidal currents inside the current ring have no external stray field and give therefore no interaction forces with external magnetic fields.

The external equilibrium magnetic field causes a much smaller lateral force than the toroidal magnetic field. Before the onset of the asymmetry of the VDE the equilibrium field in the vicinity of the vertically displaced current ring can be represented by

$$B_R \approx B_{R0} + (R - R_0) \frac{\partial B_R}{\partial R} + z \frac{\partial B_R}{\partial z}$$

$$B_\varphi = 0$$

$$B_z \approx B_{z0} + (R - R_0) \frac{\partial B_z}{\partial R} + z \frac{\partial B_z}{\partial z}$$

where $B_{R0} = -R_0 \left(\frac{\partial B_R}{\partial R} + \frac{\partial B_z}{\partial z} \right)$ is the radial magnetic field which produces the global vertical force at the plasma. This force is balanced essentially by the repelling force between the plasma and the vessel caused by the axi-symmetric part of the halo current.

When the current ring is shifted sideways by Δx and tilted about the x -axis by the angle α , the magnetic fields becomes toroidally non-uniform in the frame of the current ring. For the estimate of the lateral forces one needs only the asymmetric part of B_z :

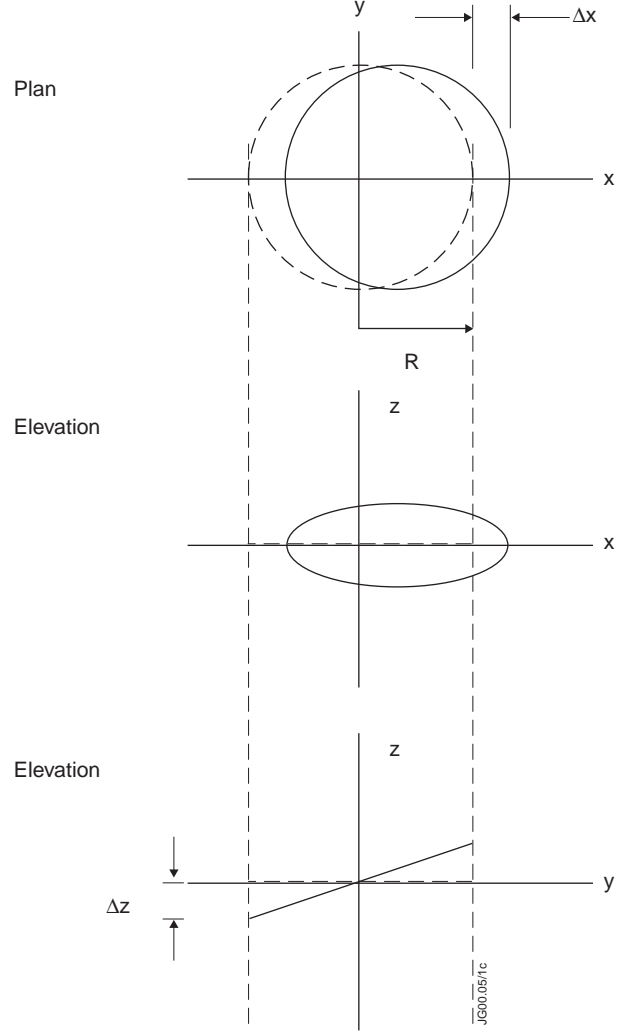


Fig. 1 Schematic of the kinked filament current representing the asymmetric plasma

$$\tilde{B}_z \approx \Delta x \frac{\partial B_z}{\partial R} \cos \varphi + \alpha \left(B_{R0} - R_0 \frac{\partial B_z}{\partial z} \right) \sin \varphi.$$

The lateral forces acting on the current ring are

$$F_x \approx \pi I_0 R_0 \frac{\partial B_z}{\partial R} \Delta x$$

$$F_y \approx \pi I_0 \left(B_{R0} - R_0 \frac{\partial B_z}{\partial z} \right) R_0 \alpha = -\pi I_0 R_0 \left(\frac{\partial B_R}{\partial R} + 2 \frac{\partial B_z}{\partial z} \right) \Delta z$$

The gradient $\partial B_z / \partial R$ is due to the quadrupolar component of the equilibrium magnetic field required to obtain a vertically elongated plasma shape as used in JET. If I_0 is taken as positive in the $+\varphi$ direction, $\partial B_z / \partial R$ must be negative. The force F_x therefore is opposite to the assumed lateral shift Δx . However, $|\partial B_z / \partial R|$ is less than 0.1 T/m for JET plasmas with plasma currents of the order of 3 MA, while the toroidal magnetic field at the plasma axis for the relevant radius during a disruption (2.5 m) is more than 3 T. Furthermore, the measured lateral shift is smaller than the asymmetric vertical displacement amplitude. Consequently the force F_x due to the equilibrium magnetic field is more than one order of magnitude smaller than the force F_x caused by the tilted current ring interacting with the toroidal magnetic field. The lateral force F_y caused by the tilt in the equilibrium field is of a similar magnitude as F_x caused by $\partial B_z / \partial R$ and Δx and causes a small deviation of the force direction from the tilt axis. Bearing in mind that the model is supposed to give only a coarse estimate of sideways forces it is justified to retain only the contribution due to the interaction with the toroidal magnetic field; this force can also be written as

$$F_x \approx \frac{\pi}{2} \Delta M_z B_0$$

where ΔM_z is the difference between the vertical current moment at $\varphi = -\pi/2$ and $\varphi = +\pi/2$.

4. EXPERIMENTAL OBSERVATIONS

Use of the magnetic force model requires that the quantity ΔM_z , the difference between the vertical current moment at opposite locations, be measured. The difference in the vertical current moments is usually close to zero because the plasma is nearly always symmetric. It is substantially different from zero only during AVDEs and goes back to zero when the plasma current disappears.

The measurement locations are indicated in figure 2. Vertical current moments are obtained by processing the signals of pick-up coils (18) and saddle loops (14) measuring the poloidal magnetic field parallel and normal to the vessel surface (figure 2). These instruments are present in four toroidal locations 90° apart from each other (in octants 1, 3, 5 and 7). The set of diagnostics in octant 3 and 7 is better (new electronics) than the set in octants 1 and 5, and in practice for only a few pulses reliable data have been collected in the old set of magnetic diagnostics.

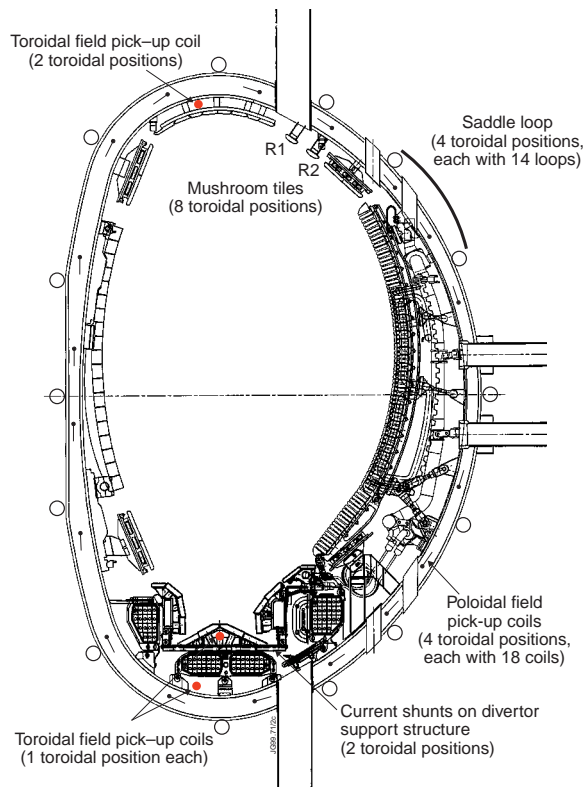


Fig. 2 Locations of the poloidal pick-up coils and saddle loops around the vessel, these magnetic diagnostics are present in 4 cross sections 90° apart. Each saddle loop covers the area between adjacent points "o" and is one octant wide. Toroidal pick-up coils are present only in two cross sections, while a pair of instrumented mushroom tiles is installed in every octant.

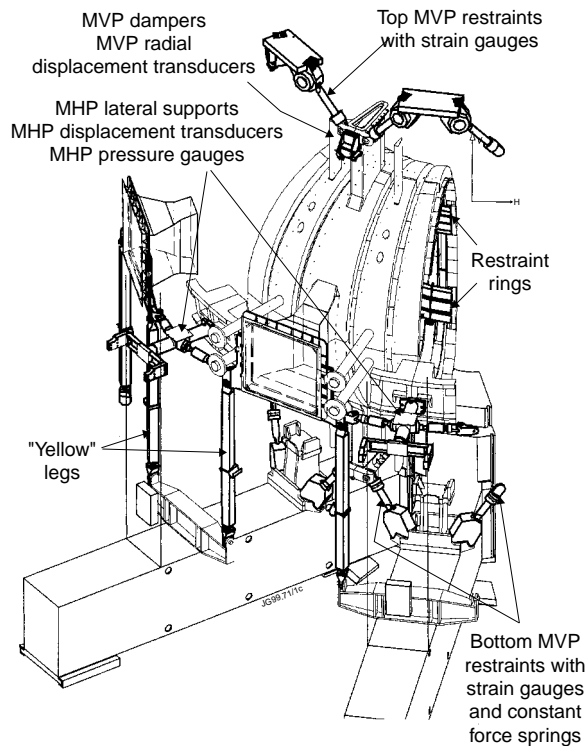


Fig. 3 Overview of the vacuum vessel supports and mechanical diagnostics.

Vessel displacements are recorded using Linear Variable Resistors (LVRs) in 8 toroidal locations, both at the top and bottom MVPs, and on the MHPs (figure 3). Displacements quoted in magnetic model validation will be restricted to those obtained from measurements at the MVPs, as these measurements have been made from the beginning of JET operation, and provide a reliable and consistent set of data.

Each of the displacement transducers has an accuracy of ~ 0.2 mm, excluding spurious signals. The average radial displacement is measured in 8 toroidal locations, therefore the accuracy of the sideways vessel displacement measurements is at least as good as the accuracy of a single transducer, while typical displacements of interest are ~ 3 -7 mm.

The uncertainty in the sideways force measurement is significantly greater, as it relies on the measurement of the asymmetry of the vertical current moment. This is estimated using a composition of many poloidal field and current measurements. The poloidal field parallel to the vessel wall is measured via pick-up coils, which have an accuracy of ~ 0.0015 T, while the normal component is measured via saddle loops, which have an accuracy of ~ 0.003 T.

The plasma vertical current moment, at each toroidal location of the magnetic diagnostics, is estimated as

$$(z_p - z_{ref})I_p = M_{z,p} \approx \frac{1}{\mu_0} \sum_{i=1}^{18} B_{\vartheta,i} z_i l_i + \frac{1}{\mu_0} \sum_{j=1}^{14} R_j B_r,j l_j \ln \frac{R_j}{R_{ref}} + \text{axi-symmetric terms}$$

where z_i are the vertical locations and l_i the mean distance to the two neighbours of the pick-up coils, R_j are the average radial locations and l_j the poloidal widths of the flux-loops and R_{ref} the reference radius and z_{ref} the reference vertical position ($z_{ref}=0$). The uncertainty of the vertical current moment measurement at one toroidal position caused by the above mentioned uncertainties of poloidal magnetic field measurements is then obtained by adding up the absolute values of all the 18+14 contributions as weighed according to the formula for the vertical current moment and this is ~40 kAm. The same uncertainty applies for the measurements at the opposite cross section. The resulting uncertainty of the vertical current moment asymmetry, taken from the difference in opposite cross sections, could be as high as ~80 kAm. In addition, the effect of other currents, such as those in the restraint rings and the divertor structure, taken as axis-symmetric without being sure they are so, has to be taken into account while making estimates of the uncertainty in the computation of the vertical current moment asymmetry. However, because the locations of greatest interest here are far away from those continuous conductors, these contributions to the error are smaller than those coming from the accuracy of the poloidal field measurements. Combining these, the total the plasma current moment asymmetry uncertainty is unlikely to be larger than 100 kA·m, and with the toroidal field at the plasma centroid being about 3 T we have a resulting uncertainty of about 300 kN in the sideways force which the magnetic model predicts.

5. LUMPED PARAMETER MECHANICAL MODEL

5.1 Introduction

Our objective is to validate the model of plasma and vessel forces by comparing observed vessel displacement histories with those which our magnetic force model would predict. This naturally requires some mechanical response model, to predict displacement dynamics as a function of magnetic force histories, and this mechanical model is outlined in the following sections.

The mechanical model employed is described in section 5.2 . There are inevitably uncertainties in the values of parameters to employ in such a model. In section 5.3 we attempt to quantify the uncertainty in the predicted displacement histories associated with plausible perturbations of parameters about their best estimate values.

5.2 The mechanical model

Mechanical models of vessel response have been the subject of prolonged development effort at JET, by many researchers, and the model we employ is built upon these [12-13-14].

The lumped parameter model used, a combination of inertias, stiffnesses and damping elements, is shown schematically in figure 4. From this model can be assembled a set of equations (1) the solution of which predicts a radial displacement history as a function of an applied lateral magnetic force.

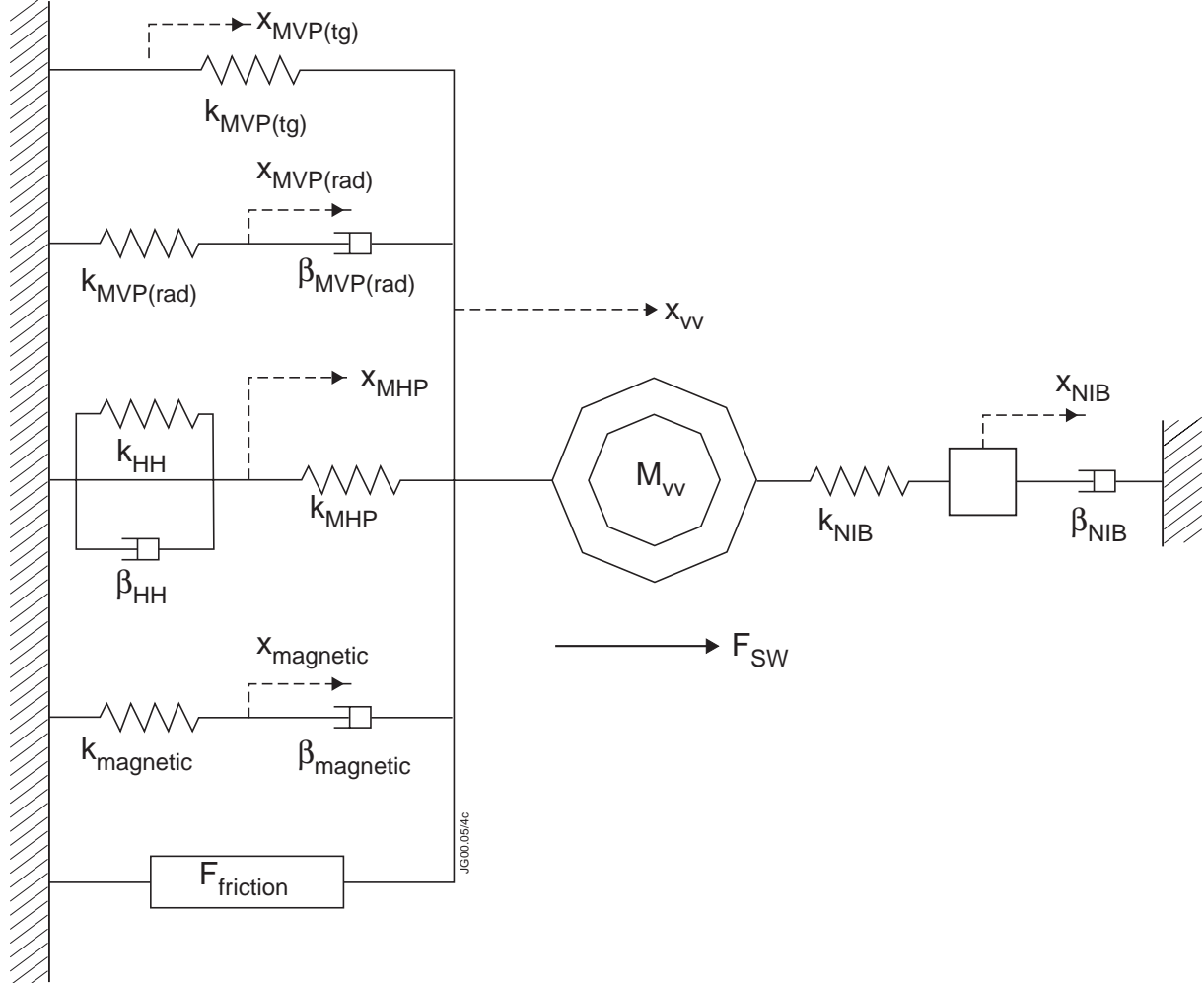


Fig. 4 The lumped parameter mechanical model

The first equation of the set refers to the Vacuum Vessel (VV), which is linked to the Neutral Injector Boxes (NIB), is mechanically restrained via the MVP dampers (acting both tangentially and radially) and via the MHP, and is magnetically restrained by the toroidal field [15]; in this equation F_{SW} is the sideways force acting on the vessel because of the plasma asymmetry and $F_{friction}$ is the friction force at the supports.

The second equation describes the behaviour of the NIB.

The third and the fourth equations are for the hydraulic dampers, respectively at the MVPs and at the MHPs. The last equation describes the magnetic restraint of the vessel. A fuller description of the mechanical model is given in the sub-section 5.3.2.

$$\left\{ \begin{array}{l} \left(M_{vv} \frac{d^2}{dt^2} + k_{MVP(tg)} \right) x + \left(M_{NIB} \frac{d^2}{dt^2} + \beta_{NIB} \frac{d}{dt} \right) x_{NIB} + k^*_{MHP} x_{MHP} + \beta_{MVP(rad)} \frac{d}{dt} x_{MVP(rad)} + \\ \quad + \beta_{mg} \frac{d}{dt} x_{mg} = F_{SW} + F_{Friction} \\ -k_{NIB} x + \left(M_{NIB} \frac{d^2}{dt^2} + \beta_{NIB} \frac{d}{dt} + k_{NIB} \right) x_{NIB} = 0 \\ -k_{MVP(rad)} x + \left(\beta_{MVP(rad)} \frac{d}{dt} + k_{MVP(rad)} \right) x_{MVP(rad)} = 0 \\ -\left(k_{HH} + \beta_{HH} \frac{d}{dt} \right) x + \left(\left(\frac{k_{HH}}{k_{MHP}} + 1 \right) \beta_{HH} \frac{d}{dt} + k_{HH} \right) x_{MHP} = 0 \\ -\beta_{mg} \frac{d}{dt} x + \left(\beta_{mg} \frac{d}{dt} + k_{mg} \right) x_{mg} = 0 \end{array} \right.$$

(1)

5.3 Parameter sensitivity and selection

Clearly, any such few-element lumped parameter mechanical model of a structure as complex as JET can only represent its behaviour approximately. In particular, even once a qualitatively correct model has been established, comprising the right assemblage of elements, there must remain considerable uncertainty over what numerical values of parameters to employ. Based on the history of the use of the such models [12-13], and on a recent work [14] aimed at systematically obtaining ‘highest confidence’ parameter sets, table 1 lists base values of parameters (masses, damping coefficients, stiffness constants and friction force).

The uncertainty on the vessel mass, and consequently on the MVP tangential stiffness and friction are mainly due to the presence of heavy diagnostics attached on the top of the vessel ports. The radial supports at the MVP have been recently refurbished and they seem to behave according to the design parameters, so no uncertainty has been placed on them. The uncertainty on the magnetic damping coefficient and stiffness constant are linked to the simplifications made to the vessel geometry and material properties in computing them. The resistance to motion of the NIB depends on the direction of the vessel displacement, so its value is uncertain. Both the structural stiffness of the MHP and the stiffness of the attached hydraulic belt are known well, while the efficiency of the dampers is less so.

There are unhelpfully many parameters to vary in the actual comparisons of measured displacements and those predicted using the magnetic model, so in the next few paragraphs we will discuss and demonstrate sensitivities. We will now compute the vessel displacement histories caused by the predicted magnetic forces, using both these base values (in table 1), and a range values around them which reflects their uncertainties.

Table 1 Lumped parameters used in the mechanical model.

definition	base value		scan values	line #
vessel mass [10^3 kg]	M_{vv}	140	+22%, +44%	1; 2
friction force [kN]	$F_{Friction}$	250	+22%, +44%	1; 2
MVP tangential stiffness [MN/m]	$k_{MVP(tg)}$	50	+22%, +44%	1; 2
MVP radial stiffness [MN/m]	$k_{MVP(rad)}$	1000	fixed	/
MVP radial damping [MN/(m/s)]	$\beta_{MVP(rad)}$	100	fixed	/
magnetic stiffness/ B_T^2 [(MN/m)/ T^2]	k_{mg}	49	-33%, +33%	3; 4
magnetic damping/ B_T^2 [(MN/(m/s))/ T^2]	β_{mg}	0.41	-33%, +33%	3; 4
NIB mass [10^3 kg]	M_{NIB}	80	-50%, +50%	5; 6
NIB stiffness [MN/m]	k_{NIB}	100	-50%	7
NIB damping [MN/(m/s)]	β_{NIB}	2	fixed	/
MHP stiffness [MN/m]	k_{MHP}	600	fixed	/
stiffness MHP hydraulic dampers [MN/m]	k_{HH}	200	fixed	/
damping MHP hydraulic dampers [MN/(m/s)]	β_{HH}	20	-50%, +50%	8; 9

A typical force history, predicted by the magnetic model, is shown in figure 5, along with the corresponding displacement history predicted by the mechanical model with the base parameter set. We will now investigate how this predicted displacement history is modified by plausible variations in the values of the principal parameters of the mechanical model. What is ‘plausible’ is necessarily subjective and in itself uncertain; we have attempted to select by engineering judgement perturbations which are of similar probability for each of the various parameters.

5.3.1 Vessel mass and support stiffness

For a given impulsive force, the vessel mass and support system stiffness together are the principal determinants of the amplitude of the first oscillation. From many analyses [14], the natural frequency of tangential oscillations of the MVP is known with some confidence (to be 3 Hz), so we need to investigate the variation in response only as the effective mass and stiffness are changed in tandem, keeping their ratio constant. Further, in order to keep the end-offset correct,

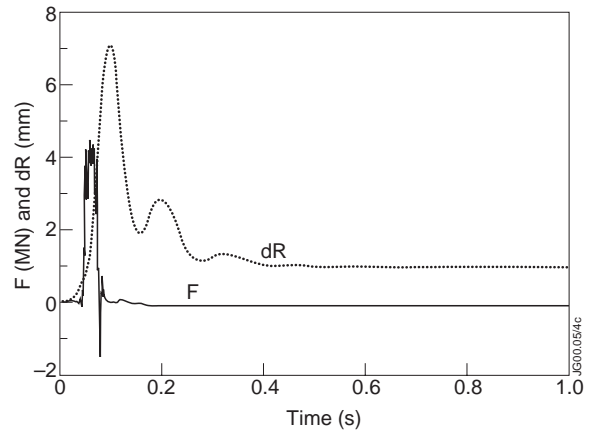


Fig. 5 The sideways force input in the lumped base-parameter mechanical model (solid line, representative of pulse 38705), which then predicts the sideways displacement (dashed line).

which is a function of the frictional forces between the vessel and its supports, the friction force also has to be changed with the vessel mass, in effect keeping the coefficient of friction constant.

The lines 2 and 3 in figure 6 show the response with the effective mass and stiffness changed simultaneously by 22% and 44%, with corresponding adjustment also of the frictional force. The peak amplitude changes by less than 5% and the time at which peak displacement is reached alters similarly little. These results provide some confidence that even quite a wide uncertainty in the mass has little effect on the

predictions of the model, and consequently on the suitability of using the lumped parameter mechanical model in assessing the validity of the analytic magnetic model in predicting the magnetic force.

5.3.2 Magnetic restraint

As the vessel moves sideways, it finds itself in a different toroidal field, but the conductive walls try to screen the field variation inside, therefore asymmetric currents are induced. These interact with the toroidal magnetic field and give a force which opposes the sideways displacement. These magnetic forces scale as the square of the toroidal field and can be represented by a viscous damping coefficient and by a stiffness constant. The normalised magnetic stiffness and damping have been computed [15] using a shell eddy current model to be 49 (MN/m)/T^2 and $0.41 \text{ (MN/(m/s))/T}^2$. Even changing them up and down by a third does not make a significant difference in the mechanical model response (figure 7).

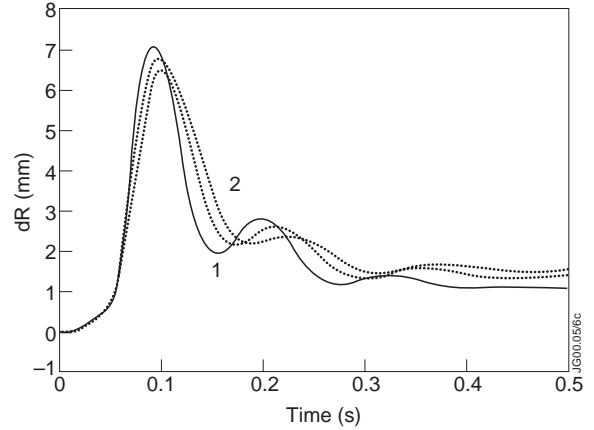


Fig. 6 Effect of the vessel mass on the displacement amplitude. The sets of parameters used are: (solid) $M_{vv}=140 \cdot 10^3 \text{ kg}$, $k_{MVP(tg)}=50 \text{ MN/m}$ and $F_{Friction}=250 \text{ kN}$; (1) $M_{vv}=180 \cdot 10^3 \text{ kg}$, $k_{MVP(tg)}=64.3 \text{ MN/m}$ and $F_{Friction}=332 \text{ kN}$; (2) $M_{vv}=220 \cdot 10^3 \text{ kg}$, $k_{MVP(tg)}=78.6 \text{ MN/m}$ and $F_{Friction}=392 \text{ kN}$.

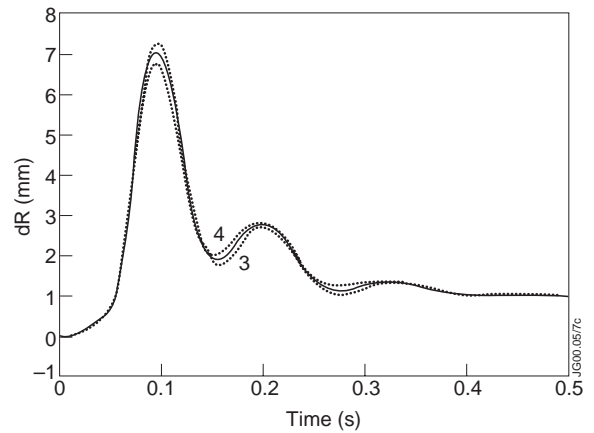


Fig. 7 Small changes are introduced by a $\pm 33\%$ variation in magnetic restraint strength. The set of parameter used are: (3) $k'_{mg}=36 \text{ (MN/m)/T}^2$ and $\beta'_{mb}=0.29 \text{ (MN/(m/s))/T}^2$; (solid) $k'_{mg}=49 \text{ (MN/m)/T}^2$ and $\beta'_{mb}=0.41 \text{ (MN/(m/s))/T}^2$; (4) $k'_{mg}=67 \text{ (MN/m)/T}^2$ and $\beta'_{mb}=0.53 \text{ (MN/(m/s))/T}^2$

5.3.3 Neutral Injector Boxes mass and stiffness and Main Horizontal Ports damping

The principal influence of the NIB mass and stiffness is in determining the shape of second peak: the mass is linked to its height and the stiffness to the depth of the valley between the two peaks (figure 8). As is seen, the effect on the amplitude of the first peak is negligible.

The effect on the response is rather stronger for the MHP damping coefficient (figure 9), especially when β_{HH} is decreased by 50% (this produces a 13% increase in the peak of the sideways displacement), while the peak amplitude changes by less than 4% if β_{HH} is increased by 50%. Such a large variation used for the MHP damping is due to the doubts on the closeness of the system to design parameters.

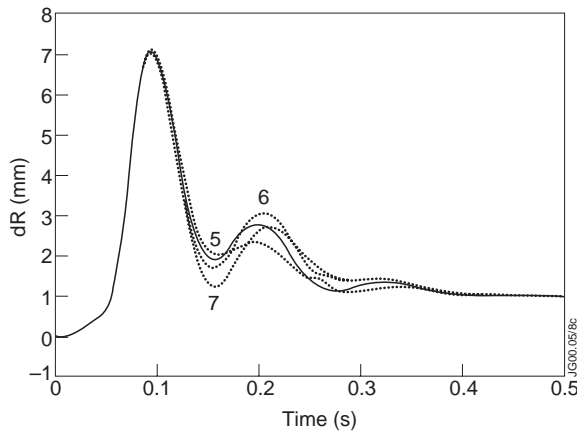


Fig. 8 NIB mass and stiffness influence on the shape of the second peak. The sets used are: (5) $M_{NIB}=40 \cdot 10^3$ kg and $k_{NIB}=100$ MN/m; (solid) $M_{NIB}=80 \cdot 10^3$ kg and $k_{NIB}=100$ MN/m; (6) $M_{NIB}=120 \cdot 10^3$ kg and $k_{NIB}=100$ MN/m; (7) $M_{NIB}=80 \cdot 10^3$ kg and $k_{NIB}=50$ MN/m.

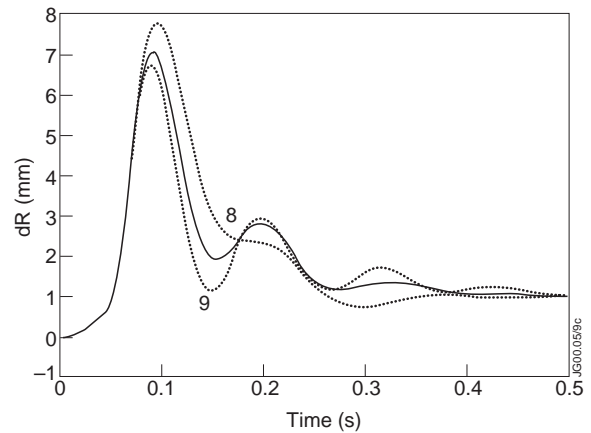


Fig. 9 Effects of varying the MHP damping by $\pm 50\%$: (8) $\beta_{HH}=10$ MN/(m/s); (solid) $\beta_{HH}=20$ MN/(m/s); (9) $\beta_{HH}=30$ MN/(m/s)

5.4 Lumped parameter mechanical model parameters: concluding remarks

It is naturally the magnitudes of the peak displacement which are of greatest interest in assessing the threat to vessel integrity posed by AVDEs. These seem to be robustly predicted by the mechanical model, regardless of which physically plausible set of model parameters are adopted. This observation provides considerable confidence in the suitability of our subsequent use of the mechanical model in the investigation of the validity of the magnetic force model.

6. MAGNETIC MODEL VALIDATION

The approach to model validation, via comparison of its prediction with experimental measurements, falls into several parts.

6.1 Displacement directions

Time integration of the sideways force, computed from the difference between the vertical current moment at opposite locations, allows the magnetic model to be used to predict the direction of

the impulse imparted to the vessel. This validation exercise has been done only for the few pulses where the data collected from the magnetic signals in octants 1 and 5 (the old set of magnetic diagnostics) were of acceptable quality.

Figure 10 shows the results of this comparison between analytical model and measurement. Once the predicted direction of the impulse has been computed, the co-ordinates have been rotated so that the sideways impulse vector points towards $\phi=0$. The measured sideways displacements, in this rotated co-ordinate system, are reasonably consistent with the direction of the impulse predicted by the simple model. The model's use of the difference between the vertical current moments in opposite cross sections is thus a valid predictor of the force direction.

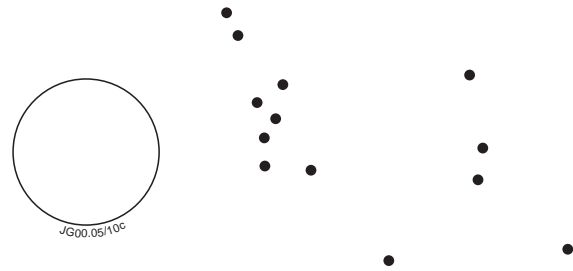


Fig. 10 Sideways displacements in a frame system rotated so that the vector force impulse points along $\phi=0$

6.2 Proportionality of predicted impulse and observed displacement

The component of the impulse predicted by the magnetic model in a given direction (from octant 5 towards octant 1, using the magnetic data from octants 3 and 7) has been compared with the component of the (peak) vessel displacement in the same direction for a set of 40 AVDEs. The results, shown in figure 11, confirm that the two quantities are proportional, indicating the model is also a valid predictor of the displacement amplitude.

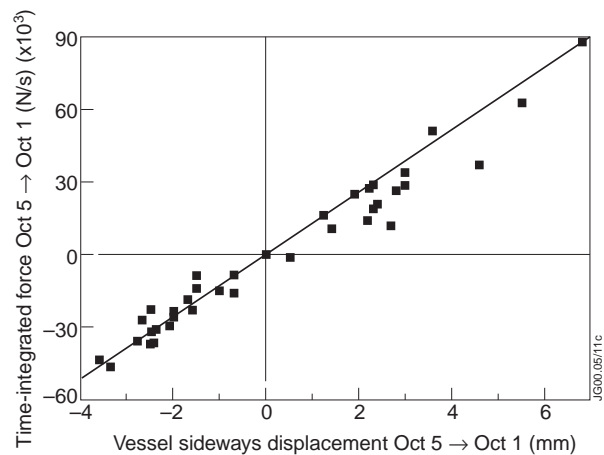


Fig. 11 Vessel sideways displacement component in direction octant 5 to octant 1 as measured at the MVPs plotted versus the sideways force impulse in the same direction as computed using the simplified magnetic model.

6.3 Magnitude of predicted and observed displacements

To perform this stage of the validation process the same sets of parameters used in the sensitivity analysis (section 5.3) are used to compute displacements histories, and these histories are those compared with displacement histories as measured at the MVPs. The input to the magnetic model is the measurement of vertical current moment differences at opposite locations, and its output a predicted lateral force history.

In figures 12a-b-c-d the force predicted by the magnetic model is shown, along with the measured displacement history, for the AVDEs of JET pulses 38705, 38070, 39207 and 39055. Our objective now is to see if the mechanical model discussed above predicts displacement histories consistent with these when given our magnetic model force history as input.

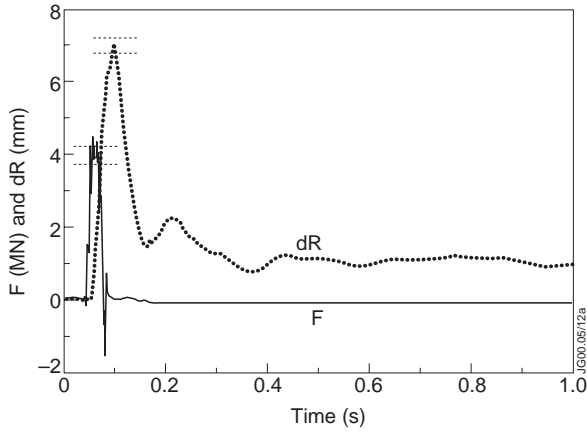


Fig. 12a Sideways force and vessel displacement for pulse 38705 (starting time 56.8 s), the dashed lines indicate the uncertainty bracket on the peak of the smoothed measured displacement and magnetic force

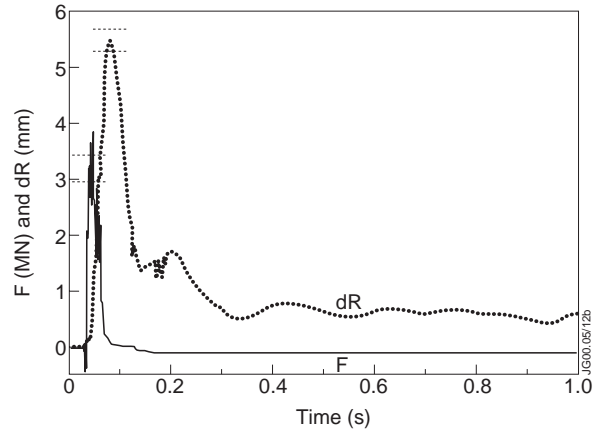


Fig. 12b Sideways force and vessel displacement for pulse 38070 (starting time 60 s), the dashed lines indicate the uncertainty bracket on the peak of the smoothed measured displacement and magnetic force

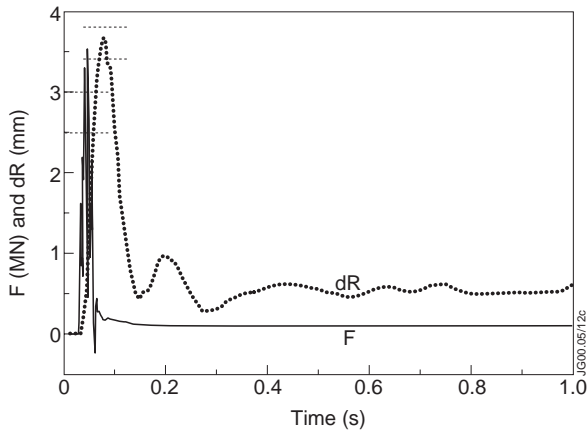


Fig. 12c Sideways force and vessel displacement for pulse 39207 (starting time 56 s), the dashed lines indicate the uncertainty bracket on the peak of the smoothed measured displacement and magnetic force

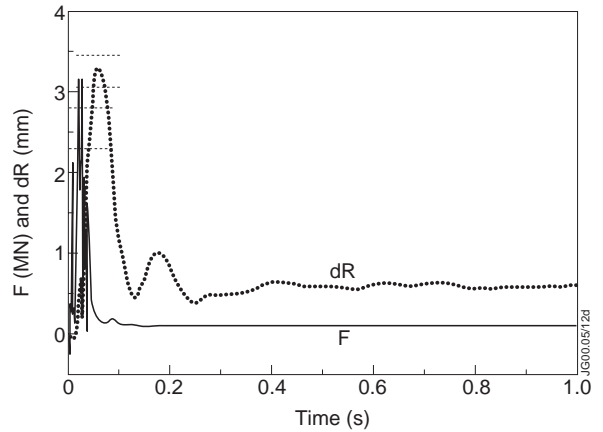


Fig. 12d Sideways force and vessel displacement for pulse 39055 (starting time 53 s), the dashed lines indicate the uncertainty bracket on the peak of the smoothed measured displacement and magnetic force

For each of the magnetic force histories in figures 12a-b-c-d a set of predicted displacement histories has been computed and plotted together with the measured ones in figures 13a-b-c-d (where labels refer to the numbered parameter groups in table 1).

In all cases the measured displacement histories lie fairly consistently within the range of displacement histories which the combined magnetic force and mechanical model predicts as the set of mechanical parameter values is scanned.

7. DISCUSSION AND CONCLUSIONS

It has been demonstrated that the force acting on the vacuum vessel during asymmetric disruptions can be estimated from readily available magnetic measurements using a simple analytical magnetic model.

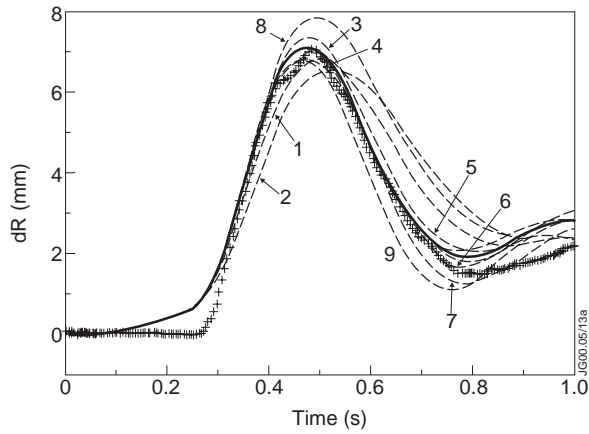


Fig. 13a Displacement history, measured (cross- points) and with parameter sets (pulse 38705)

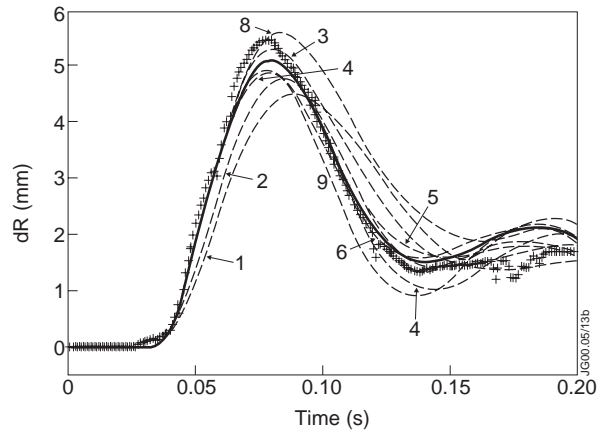


Fig. 13b Displacement history, measured (cross- points) and with parameter sets (pulse 38070)

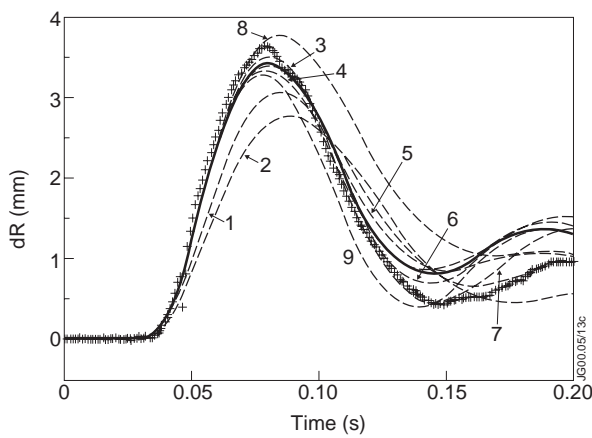


Fig. 13c Displacement history, measured (cross- points) and with parameter sets (pulse 39207)

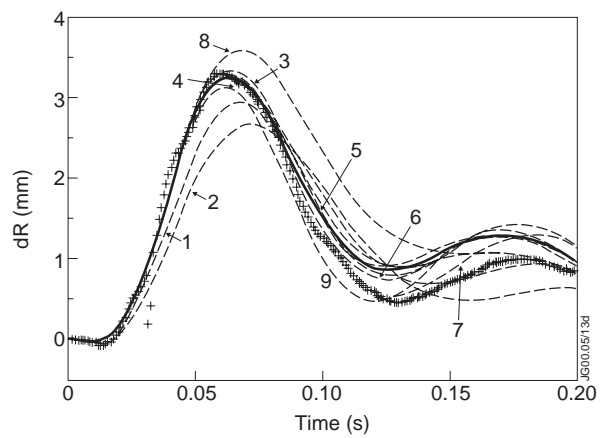


Fig. 13d Displacement history, measured (cross- points) and with parameter sets (pulse 39055)

This magnetic model has been validated. The model predictions are consistent, within an angle of $\pm 30^\circ$ with the direction of the sideways vessel displacement in the analysed set of disruptions (~ 15 events). The measured displacements have been shown to be remarkably proportional to the sideways impulses the model predicts, at least in the ~ 50 disruptions studied. The magnetic model also predicts the sideways force as a function of time. This predicted force variation gives displacement histories consistent with the measured ones, when employed in a mechanical model of the transient mechanical response of the vessel system, as shown in detail for four AVDEs for which good quality magnetic data were available.

We conclude that the simple magnetic force model presented here is valid, and can provide a general tool to assess the potential harm of AVDEs.

One immediate and simple observation from the magnetic model is that the sideways force scales with the product of the plasma current and the toroidal field. The maximum amplitude of the vertical position asymmetry is limited by the space available for the vertically displaced plasma to tilt while preserving enough area to sustain its current. In addition the survival of the unstable displaced plasma is limited in time by the in-flux of impurities, which increases the

radiation cooling and the plasma resistivity. Consequently also the maximum potential sideways displacement to a first approximation scales as the product of the plasma and the toroidal field. This recipe is now used at JET to assess *a priori* the hazards of performing high current and high field pulses when they are known to be likely to disrupt.

Although developed for and validated on JET, the magnetic force model described here is of general applicability to all tokamak devices subject to a significant $m=1/n=1$ mode.

8. ACKNOWLEDGEMENTS

We gratefully acknowledge the useful discussions with Drs T. Raimondi and D. Ward.

REFERENCES

- [1] J. Wesley, N. Fujisawa, S. Ortolani, S. Putvinskij, M.N. Rosenbluth, Disruption, Vertical Displacement Event and Halo Current Characterisation for ITER, Proc. 16th IAEA Conf., Montreal (1996) vol. 2, p. 971
- [2] Y. Neyatani, R. Yoshino, T. Ando, Effect of Halo Current and its Toroidal Asymmetry during Disruptions in JT60-U, Fusion Technol. 28 (1995) 1634
- [3] G.G. Castle, A.W. Morris, D.A. Gates, C.G. Gimblett, M. Valovic, Halo Currents and VDEs in COMPASS-D, Proc. 16th IAEA Conf., Montreal (1996), vol. 2
- [4] R.S. Granetz, I.H. Hutchinson, J. Sorci, B. Labombard and D. Gwinn, Disruptions and halo currents in Alcator C-MOD, Nucl. Fusion 36 (1996) 545
- [5] T.E. Evans, A.G. Kellman, D.A. Humphreys, M.J. Shaffer, P.L. Taylor, D.G. Whyte, T.C. Jernigan, A.W. Haytt, R.L. Lee, Measurements of non-axisymmetric halo currents with and without ‘killer’ pellets during disruptive instabilities in DIII-D tokamak, J. Nucl. Mater., vol. 241-243 (1997) 606
- [6] O. Gruber et al., MHD stability and disruption studies in Asdex-upgrade, Proc. 16th IAEA Conf., Montreal (1996) vol. 1, p. 359
- [7] V. Marchese et al., Enhancement of JET Machine Instrumentation and Coil Protection Systems, Proc. 19th Symposium on Fusion Technology, Lisbon (1996) vol. 1, p. 747
- [8] P. Noll et al., Present Understanding of Electromagnetic Behaviour during Disruptions at JET, Proc. 19th Symposium on Fusion Technology, Lisbon (1996) vol. 1, p. 751
- [9] T.H. Jensen, M.S. Chu, Long-term development of elongated tokamak plasmas after failure of feedback stabilization, Phys. Fluids B, vol 1 (1989) p. 1545
- [10] A. Caloutsis, C.G. Gimblett, A novel plasma-wall instability and the distribution of halo currents in tokamaks, Nucl. Fus. (1998) vol. 38, p. 1487
- [11] R Litunovsky, *The observation of phenomena during plasma disruption and the interpretation of the phenomena from the point of view of the toroidal asymmetry of forces*, JET internal report (contract No. JQ5/11961), 1995
- [12] A. Kaye, Sideways Displacements of the Torus, Internal JET report (Annex 4 in the Joint

JET-JSC-RAG report to the 65th JET Scientific Council, March 1997)

- [13] T. Raimondi, Some Results from the Sideways model, Internal JET report (Annex 5 in the Joint JET-JSC-RAG report to the 65th JET Scientific Council, March 1997)
- [14] M. Buzio, Structural Effects of Plasma Instabilities on the JET Tokamak, PhD thesis, Imperial College, London (1998)
- [15] V. Riccardo, Asymmetric Vertical Displacement Events in JET, PhD thesis, Imperial College, London (1998)